Analysis of the factors affecting the magnetic characteristics of nano-Fe$_3$O$_4$ particles

LI JianLing*, LI DeCai*, ZHANG ShaoLan, CUI HongChao & WANG Cui

School of Mechanical, Electronic and Control Engineering, Beijing Jiaotong University, Beijing 100044, China

We prepared Fe$_3$O$_4$ nanoparticles using chemical coprecipitation and studied the factors affecting the magnetic characteristics of nano-Fe$_3$O$_4$ particles. We identified four factors and three levels of an orthogonal experiment and investigated these four factors that affect the magnetic characteristics of the Fe$_3$O$_4$ particles. We obtained important information from this investigation. The Fe^{3+} to Fe^{2+} molar ratio, the iron precursor salt, the amount of surfactant and the amount of alkali were found to be important. We also studied the influence of the order of alkali and surfactant addition, the aging time and the stirring speed on the magnetic characteristics of the nano-Fe$_3$O$_4$ particles. The Fe$_3$O$_4$ preparation process was also analyzed.

nanomagnetic fluid, nano-Fe$_3$O$_4$ particles, saturation magnetization, influencing factors

Nanomagnetic fluids are a new type of nanofunctional material that consists of nanomagnetic particles coated with surfactant molecules and dispersed in a liquid-based composition containing a stable colloidal system. Nanomagnetic fluid has mobility and magnetic. Both the magnetic and liquid components are in the same material so the nanomagnetic fluid has many unique properties, such as mechanical, magnetic, optical, catalytic and acoustic properties, etc. And nanomagnetic fluid has a wide range of applications, at present it has applications in industrial, military, aerospace, and many other areas. For the nanomagnetic fluid research, China is relatively backward in the United States, Russia and Japan, etc., needs further research and development. The nanomagnetic fluid is contained in a liquid-based magnetic particle and surfactant composition, as shown in Figure 1 [1].

Nanomagnetic particles are an important component of magnetic fluid and liquid-based being one by the role of surfactant [2]. And nanomagnetic fluid can also exist in
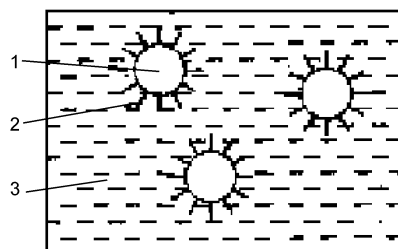

Figure 1   Schematic composition of a nanomagnetic fluid. 1, Magnetic particle; 2, surfactant; 3, liquid-base.

long-term stability even in the gravity field, electric field and magnetic field, not produce precipitation and separation, so it is practical [1,2]. The nature and content of the nanomagnetic particles determines the magnetic properties of the magnetic fluid and this is important in the preparation of an excellent magnetic liquid with wide potential application. The magnetic properties of a nanomagnetic fluid are derived from nano-Fe$_3$O$_4$ magnetic particles. These magnetic nanoparticles and their magnetic properties have very important significance, and they are the focus of this study.

*Corresponding authors (email: 07116303@bjtu.edu.cn; dcli@bjtu.edu.cn)

1 Experimental materials and methods

1.1 Reagents and equipment

The main reagents that we used were $FeCl_3 \cdot 6H_2O$ (analytically pure), $FeCl_2 \cdot 4H_2O$ (analytically pure), ascorbic acid (analytically pure), ammonia (analytical pure), oleic acid (analytically pure), distilled water and silver nitrate (analytically pure).

The main instruments that we used were an LP3102 electronic balance, HH-2 type digital constant temperature water bath, D-8401-WZ type multi-function electric mixer, fume hood, ZK-82B type vacuum drying oven, 2XZ-2 type rotary vane vacuum pump, WS70-1 type infrared rapid dryer, LDJ9600 strong magnetic field vibrating sample magnetometer and a H800 transmission electron microscope.

1.2 Preparation and process

The general process for the preparation of nano-Fe_3O_4 particles by chemical coprecipitation included using $FeCl_2 \cdot 4H_2O$ and $FeCl_3 \cdot 6H_2O$ as raw materials and NaOH (or $NH_3 \cdot H_2O$) as precipitating agents. A specific proportion of Fe^{3+} and Fe^{2+} was used in solution and by reaction with OH^-, Fe_3O_4 magnetic particles of about 10 nm were prepared [3–6]. The reaction mechanism is shown in eqs. (1) and (2). And the preparation process is shown in Figure 2:

$$Fe^{2+} + 2Fe^{3+} + 8OH^- \rightarrow Fe_3O_4 + 4H_2O \quad (1)$$

$$FeCl_2 + 2FeCl_3 + 8NaOH = Fe_3O_4 + 8NaCl + 4H_2O \quad (2)$$

Saturation magnetization of Fe_3O_4 nanoparticles is the most important performance indicator. For the preparation of nano-Fe_3O_4 particles many factors determine the characteristics of the nano-Fe_3O_4 magnetic particles [7–12] such as the Fe^{3+} to Fe^{2+} molar ratio, the Fe concentration of the salt solution, the amount of alkali, the amount of surfactant, the order of alkali and surfactant addition, the reaction onset temperature, the curing temperature, the stirring speed and the aging time. To study these factors, we summarized the preparation conditions based on their impact on the magnetic properties of the Fe_3O_4 particles. For the four factors: Fe^{3+}/Fe^{2+} molar ratio, amount of deionized water amount, amount of alkali and amount of surfactant, we designed a four-factor three-level orthogonal $L_9(3^4)$, experimental table as shown in Table 1 [13–17]. For our experiment, the alkali was ammonia and the surfactant was oleic acid. For the reaction, we added ammonia to the precursor solution and then added oleic acid.
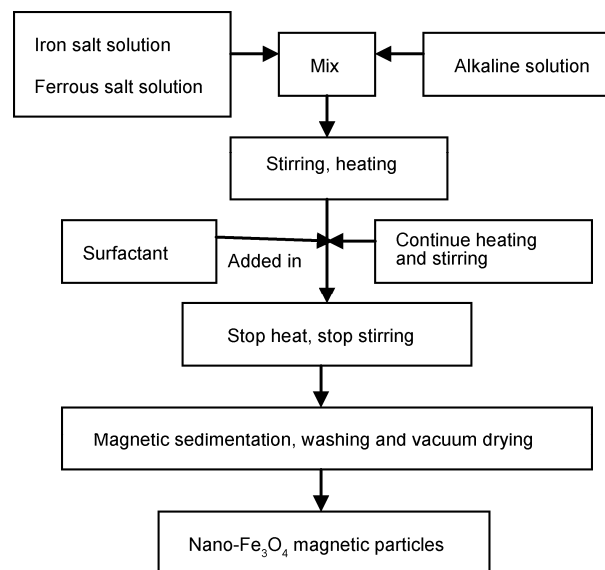

Figure 2 Flowchart for the preparation of the nano-Fe_3O_4 magnetic particles.

This combination represents a set of nine experiments: $A_1B_1C_1D_1$, $A_1B_2C_2D_2$, $A_1B_3C_3D_3$, $A_2B_1C_2D_3$, $A_2B_2C_3D_1$, $A_2B_3C_1D_2$, $A_3B_1C_3D_2$, $A_3B_2C_1D_3$, $A_3B_3C_2D_1$.

A specific temperature was used for each experiment and the precursor solution was rapidly stirred ($FeCl_3$ and $FeCl_2$ solution) while ammonia was added quickly. The solution was rapidly heated to temperature and the stirring speed increased. The temperature was adjusted over time when adding oleic acid to maintain a constant temperature and a constant stirring speed was used to enable the complete reaction of the Fe_3O_4 nanoparticles.

Our experimental results were analyzed using the orthogonal comparison table (Table 2). The process of coprecipitation generated Fe_3O_4 particles and the effect of these factors on the magnetic properties of the obtained Fe_3O_4 particles were determined by comparing the experimental factors [18,19].

From Table 2, the four factors that were selected evidently influence the saturation magnetization of the nano-Fe_3O_4 particles. The size of the factors follows the order: D>A>B>C. The first is the Fe^{3+} to Fe^{2+} molar ratio, the second is the amount of deionized water (reaction precursor iron salt concentration), the third is the amount of surfactant and the last is the amount of alkali. The optimal conditions are $D_2A_2B_1C_3$ where the Fe^{3+} to Fe^{2+} molar ratio is 1.75, obtained using 0.02 mol $FeCl_3 \cdot 6H_2O$ in 200 mL deionized water to give a 0.1 mol/L solution, 0.5 mL

Table 1 Orthogonal table of the preparation conditions for the nano-Fe_3O_4 particles

Level	A Amount of deionized water (mL)	B Amount of oleic acid (mL)	C Amount of ammonia (mL)	D Fe^{3+}/Fe^2 molar ratio
1	100	0.5	10	1.60
2	200	1.0	20	1.75
3	400	1.5	30	1.90

Table 2　Orthogonal test results

Experiment	A Amount of deionized water (mL)	B Amount of oleic acid (mL)	C Amount of ammonia (mL)	D Fe^{3+}/Fe^{2+} molar ratio	Saturation magnetization (emu/g)
1	1	1	1	1	52.73
2	1	2	2	2	60.98
3	1	3	3	3	52.11
4	2	1	2	3	64.21
5	2	2	3	1	57.83
6	2	3	1	2	64.72
7	3	1	3	2	69.47
8	3	2	1	3	54.40
9	3	3	2	1	53.54
K_1	165.82	186.41	171.85	164.10	
K_2	186.76	173.21	178.73	195.17	
K_3	177.41	170.37	179.41	170.72	
k_1	55.27	62.14	57.28	54.70	
k_2	62.25	57.74	59.58	65.06	
k_3	59.14	56.79	59.80	56.91	
R	6.98	5.35	2.52	10.36	

a) K is the number of occurrences of each factor and for the obtained results such as $L_9(3^4)$, the first factor is an average of 3, K_1 is the result of these three values and k_1 is the expressed average, while R is the expressed extreme.

surfactant and 30 mL ammonia.

　Based on the previous set of experiments, we undertook several additional experiments: (i) To determine the best order of surfactant and alkali addition at a specific stirring speed. The experiment was initiated at 60°C in the water bath and the iron salt solution was treated using ammonia first and then oleic acid was added. The solution was then heated to 80°C and kept at that temperature for 100 min. The next experiment was also started at 60°C and oleic acid was added to the iron salt solution first followed by the addition of ammonia and heating at 80°C for 100 min. A third experiment was started at 60°C, ammonia was added to the iron salt solution ammonia and then heating at 80°C with instant addition of oleic acid; this reaction was conducted for 100 min. (ii) To investigate different aging times, experiments were started at 60°C at a certain stirring speed and ammonia was added quickly to the iron salt solution, the mixing speed was increased, and the heating temperature was increased to 80°C and kept there for 10 min after the addition of oleic acid. Constant temperatures were maintained for 30 min, 60 min and 120 min. (iii) To investigate different stirring speeds, the experiments were started at 60°C and at a stirring speed of 150 r/min. Ammonia was quickly added to the iron salt solution and the mixing speed was increased while the heating temperature was kept at 80°C for 10 min. Oleic acid was then added and the reaction was allowed to continue for 90 min at stirring speeds of either 255 r/min or 205 r/min.

2　Results and discussion

2.1　Characterization of the nano-Fe_3O_4 particles

Photographs of the obtained nano-Fe_3O_4 magnetic particles are shown in Figure 3. The 5th product had the worst black degree and was a brown powder that was very dry and had

less surfactant. The coating of those particles was not complete and some were oxidized. The 9th product was the blackest and was sticky but not too dry and contained more surfactant. Its particles were coated well with almost no oxidation having occurred but the reunion was serious. The other products are black-gray dry powders of which the 3rd was blacker than the 7th but it was agglomerated and the 7th was a dry powder. The amount of oleic acid on the 3rd was 1.5 mL and the amount of oleic acid on the 7th was 0.5 mL.

　Magnetic nanoparticles have excellent surface energy and the thermodynamic instability gradually becomes larger because of the drying process and the reunion. Magnetic
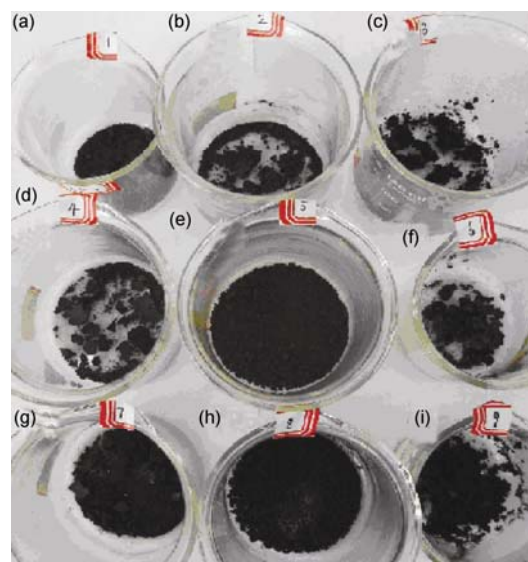
Figure 3　Photos of the orthogonal product Fe_3O_4 nanoparticles. (a) Experiment 1, $A_1B_1C_1D_1$; (b) experiment 2, $A_1B_2C_2D_2$; (c) experiment 3, $A_1B_3C_3D_3$; (d) experiment 4, $A_2B_1C_2D_3$; (e) experiment 5, $A_2B_2C_3D_1$; (f) experiment 6, $A_2B_3C_1D_2$; (g) experiment 7, $A_3B_1C_3D_2$; (h) experiment 8, $A_3B_2C_1D_3$; (i) experiment 9, $A_3B_3C_2D_1$.

cross-linking between particles occurs in a chain or network structure especially on the particle surface and free water molecules are adsorbed to form hydrogen bonds with free hydroxyls. During the drying process, this hydrogen bonding leads to bridging because adjacent particles are brought closer to a particle's surface and further dehydration makes it difficult to form chemical bonds while the generated particles disperse into aggregates. Some nanomagnetic powders with special magnetic properties promote aggregation between particles [20].

We observed the Fe_3O_4 products. (i) The order of reactant addition affects them. The products are dry powders and by adding ammonia at 60°C and oleic acid at 80°C, the obtained product is dark brown while the other two products are black-gray. (ii) The aging time also has an effect as the products are dry black powders and the product obtained at constant temperature after a 30 min reaction is the blackest, while the product obtained after 120 min is less black and this shows that a long aging time is conducive to oxidation. This oxidation affects the purity of the resulting powder but over a short aging time, co-precipitation is not complete. (iii) The product obtained at a stirring speed of 255 r/min is a black brown powder while at 205 r/min the product is black. Faster stirring results in better contact between the reactants and uneven local concentrations are avoided so that nuclei are generated and they grow to a small but uniform size [21]. Too quick a stirring speed will promote partial oxidation.

We used a vibrating sample magnetometer to determine the saturation magnetization of the Fe_3O_4 nanoparticles. From the test results, the saturation magnetization of the nano-Fe_3O_4 particles is large at 45–70 emu/g at equilibrium and when the solution is stable. For this set of orthogonal products, the highest saturation magnetization was found for the 7th product and was 69.47 emu/g with the lowest found for the 3rd at 52.11 emu/g. The amount of oleic acid used for the 3rd was 1.5 mL and the amount of oleic acid used for the 7th was 0.5 mL. An increase in the amount of surfactant leads to a decrease in the saturation magnetization of the Fe_3O_4 particles. The saturation magnetization curves for the group of nine Fe_3O_4 nanoparticle experiments is shown in Figure 4. The saturation magnetizations of the nano-Fe_3O_4 particles are large while the stubborn magnetic and remanence properties indicate that the products are superparamagnetic Fe_3O_4 particles.

The saturation magnetization curves show that the order of addition affects the Fe_3O_4 particles, as shown in Figure 5. The saturation magnetization of the Fe_3O_4 nanoparticles produced by adding ammonia at 60°C followed by adding oleic acid and then heating to 80°C was found to be 47.33 emu/g. The product obtained by adding oleic acid at 60°C followed by adding ammonia and then heating to 80°C gave a value of 50.95 emu/g. The product obtained by adding ammonia at 60°C and heating to 80°C before adding oleic

acid shows the highest saturation magnetization of 55.51 emu/g. The reaction undertaken by adding ammonia to the iron salt solution at 60°C first and then heating to 80°C upon which oleic acid was added to obtain the nano-Fe_3O_4 magnetic particles gave better results.

The saturation magnetization curve of the aging time was affected by the type of Fe_3O_4 particles produced, as shown in Figure 6. The saturation magnetization was close for the products produced at constant temperature over 30 min, 60 min and 120 min, and the values were 58.55 emu/g, 57.47 emu/g and 56.14 emu/g, respectively. A specific aging time contributes to the whole lattice of Fe_3O_4 having ultrafine and magnetic properties [22]. By repeat experiments, we determined that the optimum aging time is between 40–130 min.
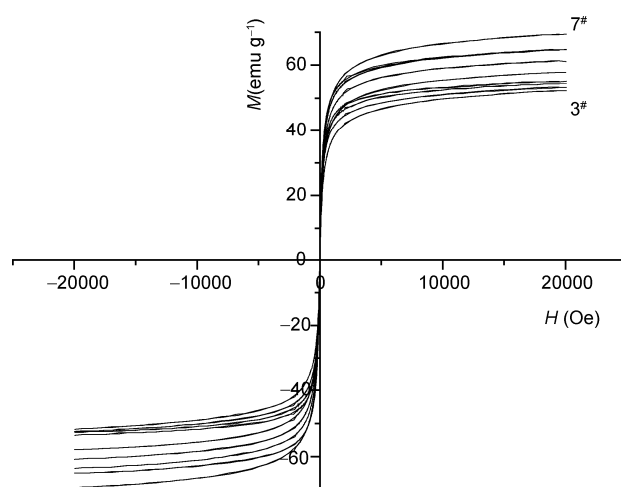
Figure 4   Saturation magnetization curves of the orthogonal Fe_3O_4 nanoparticles.
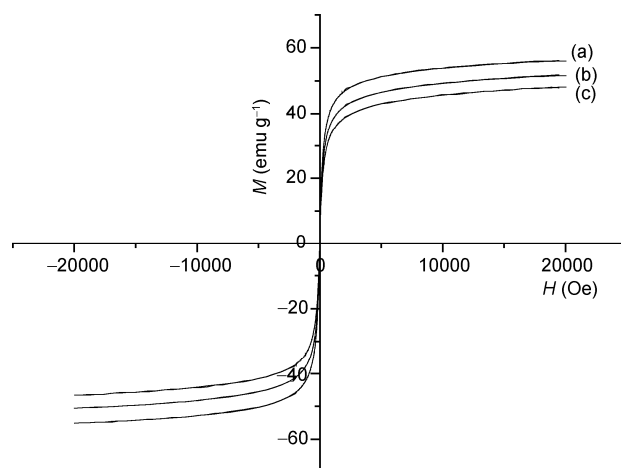
Figure 5   Saturation magnetization curves for the order of reactant addition. (a) at 60°C with ammonia addition and heated to 80°C with oleic acid addition; (b) at 60°C by oleic acid addition followed by ammonia addition and heating to 80°C; (c) at 60°C by ammonia addition followed by oleic acid addition and heating to 80°C.
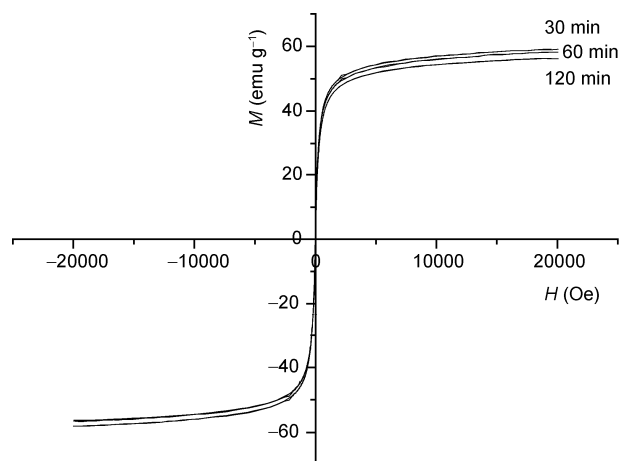
Figure 6 Saturation magnetization curves showing the effect of aging time on the Fe$_3$O$_4$ particles.
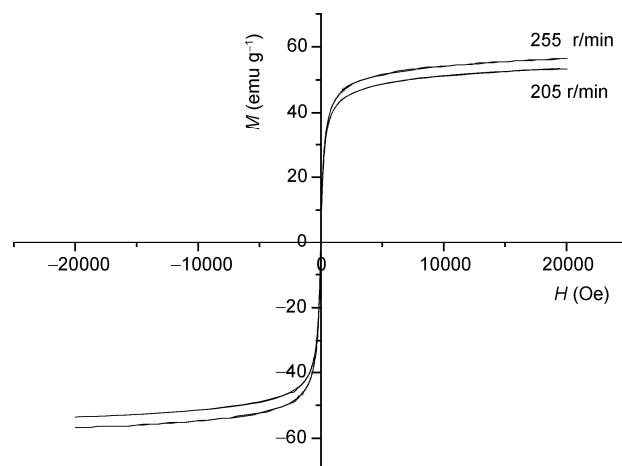
Figure 7 Saturation magnetization curve of stirring speed that affected the Fe$_3$O$_4$ particles.

Saturation magnetization curves also show that stirring speed affects the produced Fe$_3$O$_4$ particles and is shown in Figure 7. The product obtained using a stirring speed of 255 r/min had a saturation magnetization of 56.42 emu/g and the product obtained using a stirring speed of 205 r/min had a value of 53.23 emu/g. Therefore, as the stirring speed increases the saturation magnetization of the Fe$_3$O$_4$ nanoparticles increases and the optimum stirring speed is close to 300 r/min.

We analyzed the nano-Fe$_3$O$_4$ particles from the 3rd and 7th sets by transmission electron microscopy (TEM) because the saturation magnetization of the 3rd Fe$_3$O$_4$ set of nanoparticles was the lowest and the 7th Fe$_3$O$_4$ was the highest; the results are shown in Figure 8. The particle sizes appear to be uniform with spherical or nearly spherical shapes. The 3rd Fe$_3$O$_4$ set of particles were all smaller than 10 nm and the majority were around 7~8 nm. The 7th set of

Fe$_3$O$_4$ particles were about 10 nm in size but mostly below 10 nm and the largest particles were less than 13 nm. The 3rd set of particles is smaller than the 7th but agglomeration in the 3rd set is more prevalent. The amount of surfactant on the 3rd is higher than that on the 7th and the amount of oleic acid on the 3rd is 1.5 mL while that on the 7th is 0.5 mL. Therefore, the addition of surfactant has a role in inhibiting the growth of the magnetic particles but excess surfactant particles do recombine.

The attraction between magnetic particles in the magnetic fluid causes particle agglomeration while settling occurs because of gravity. However, the thermal motion of Brownian particles can prevent the settling caused by gravity. In general, for particle sizes less than 20 nm Brownian motion can overcome the gravitational field and this results in uneven settlement, assuming a single size for the spheri-
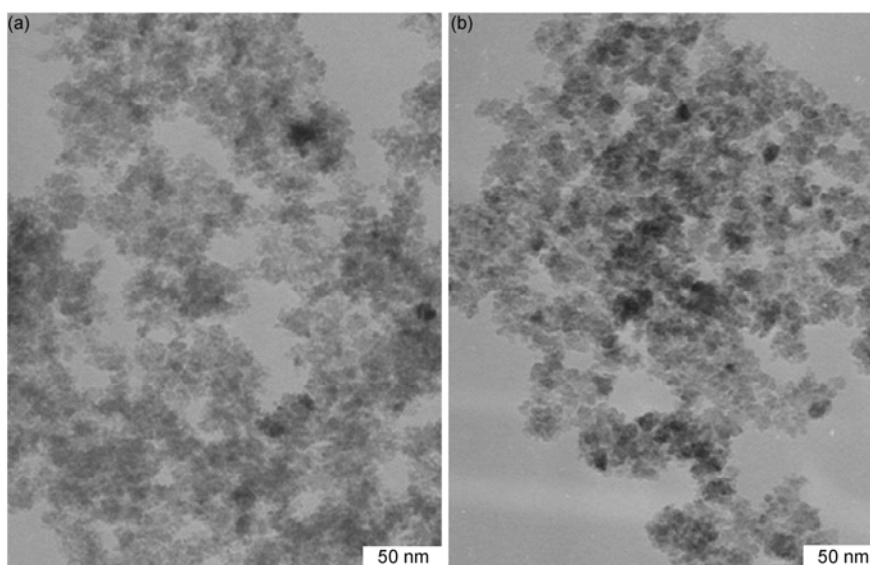

Figure 8 Transmission electron microscopy (TEM) photographs of Fe$_3$O$_4$ nanoparticles. (a) The 3rd ample; (b) the 7th sample.

cal particles in a liquid-based Brownian motion environment [23]. Because our nano-Fe_3O_4 particles are about 10nm, this requirement is met.

2.2 Mechanism of the nano-Fe_3O_4 particles

Fe_3O_4 is in fact not a mechanical mixture of FeO and Fe_2O_3 but an acid-type iron ferrous salt and its molecular structure is $Fe^{2+}(Fe^{3+}O_2)_2$. Weak ionization occurs in aqueous solution [24], as shown in eq. (3):

$$Fe(FeO_2)_2 + 2H_2O \leftrightarrow Fe(OH)_2 + 2H^+ + 2(FeO_2)^- \quad (3)$$

Fe_3O_4 magnetic particles have a face-centered cubic crystal structure. In the anti-spinel structure of Fe_3O_4 ferrite, oxygen ions are present in the skeleton consisting of face-centered cubic packing. The unit cell contains 32 oxygen ions in space to form a gap of 64 four-decent (decent space for each four by four neighboring oxygen ions, known as the A-bit) and 32 eight-decent (each 8-sided gap has six neighboring oxygen ions, known as the B-bit). Each cell consists of 96 lattices, in which the metal ions in the A-bit are 8 and in the B-bit are 16. The A position and B position of the magnetic ions that have opposite magnetic moment orientations are parallel [25]. The Fe_3O_4 lattice with high saturation magnetization of the Fe_3O_4 nanoparticles is shown in Figure 9.

Chemical coprecipitation of nano-Fe_3O_4 magnetic particles includes early and late reaction stages. The initial reaction involves a Fe^{3+}–Fe^{2+} polymer intermediate material and a phase change mechanism accompanied by initial nucleation and growth of Fe_3O_4. Adding a precipitation agent (ammonia) generates a large amount of black net floc product and the reaction process is shown in eq. (4).

$$Fe^{3+} + Fe^{2+} + OH^- \rightarrow Fe^{3+} - Fe^{2+} \text{ Polymer} \quad (4)$$
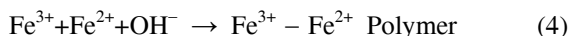
The initial high concentration of hydroxyl groups formed by a large number of hydroxyl and oxygen bridges results in the product initially being in a scattered state at the interface and a high degree of cross-linking activity is evident. From the hydrolysis and the decrease in Fe^{3+} and Fe^{2+}, we analyzed the formation of Fe_3O_4 precipitates and found that
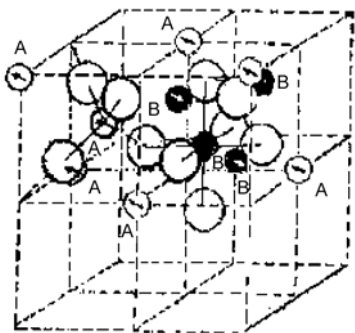
Figure 9 Fe_3O_4 lattice diagram.

Fe^{2+} weakly hydrolyzes in water, and the hydrolysis equation can be written as:

$$Fe^{2+} + 2H_2O \leftrightarrow Fe(OH)^+ + H_3O^+ \quad (5)$$

Fe^{3+} is more prone to hydrolysis than Fe^{2+}. The hydrolysis products can be further reduced in the presence of multiple bases. In fact, Fe^{3+} is a six coordinated hydrated complex ion $[Fe(H_2O)_6]^{3+}$ under these conditions and the final hydrolysis balance can be expressed as eqs. (6), (7):

$$[Fe(H_2O)_6]^{3+} + H_2O \leftrightarrow [Fe(H_2O)_5OH]^{2+} + H_3O^+ \quad (6)$$

$$[Fe(H_2O)_5OH]^{2+} + H_2O \leftrightarrow [Fe(H_2O)_4(OH)_2]^+ + H_3O^+ \quad (7)$$
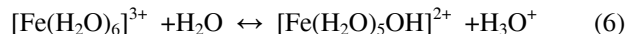
Alkaline hydrolysis of the ion balance can occur by the condensation of a polynuclear complex and the ion reactivity is

$$2[Fe(H_2O)_5(OH)]^{2+} \leftrightarrow [Fe(H_2O)_4Fe(H_2O)_4(OH)_2]^{2+}$$
$$+ 2H_3O^+ \quad (8)$$
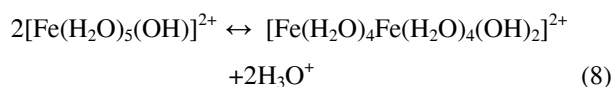
When the system has a large amount of Fe^{2+} and Fe^{3+}, the hydrolysis equilibrium formed by their presence may result in a more complex network structure. $(Fe-OH)^+$ and Fe^{2+} can partially substitute for Fe^{3+}, which is formed by Fe_3O_4. When the OH^- concentration increases, hydrogen bridges produce dual-core complexes and more complicated condensation occurs to form a colloidal solution. Finally, the Fe^{2+} and Fe^{3+} ratio in $mFe_2O_3 \cdot nFeO$ precipitation results in high purity Fe_3O_4 precipitation when $m=n$. When m and n are not equal, excess Fe^{3+} or Fe^{2+} ions will precipitate as the iron oxides, FeO or Fe_3O_4, respectively. However, the formation of impure FeO reduces the lattice integrity of Fe_3O_4 and the magnetic intensity of the mixture of FeO and Fe_3O_4 is lower than that of pure Fe_3O_4. These two factors lead to a decrease in the saturation magnetization [26,27]. The control of Fe^{3+} and Fe^{2+} at a molar ratio of 1.75 can give better results. Theoretically the Fe^{3+}/Fe^{2+} molar ratio should be 2 but in this study no inert gas was used and the solution thus had direct contact with air. Fe^{2+} easily oxidizes to Fe^{3+} under these conditions. In addition, with conditions where Fe^{2+} is easily oxidized, $\alpha-FeOOH$ forms under alkaline conditions and this reduces the purity of the product [28]. Therefore, we used excess Fe^{2+} to compensate for this deficiency.

The precursor iron salt concentration directly affects the reaction rate, the particle size and the magnetic properties of the reaction products. At a higher precursor concentration a faster reaction occurs, the product is larger, the product concentration is higher, particle growth and aggregation is more likely and no improvement in the magnetic particles is evident [24]. After an analysis and comparison of the experimental results, we selected a Fe^{3+} salt solution precursor concentration of 0.1 mol/L and the production of nano-Fe_3O_4 magnetic particles was relatively good. In accordance with the reaction equation, when using a molar ratio of $FeCl_3 : FeCl_2 : NH_4OH$ of 2:1:8 and 0.02 mol $FeCl_3 \cdot 6H_2O$ then the corresponding theoretical amount of

ammonia water (content 25%–28%) should be about 11 mL. An environment that is too alkaline is conducive to the formation of nano-Fe_3O_4 particles and ammonia is likely to be volatile. Therefore, in the actual preparation process we used excess ammonia to ensure a co-precipitation reaction. Using 30 mL of ammonia, we found that the preparation of nano-Fe_3O_4 magnetic particles was relatively good.

The reaction consists of nucleation and Fe_3O_4 crystal growth. These two processes determine the relative speed of the direct formation of magnetic particles. When the solution is oversaturated, crystallization takes place from solution by the formation of nuclei and solute diffusion through the crystal surface of the retention layer results in continuous deposition on the crystal surface, which promotes grain growth [29]. Fe_3O_4 nucleation and grain growth is the main process and ultimately the generation of nano-Fe_3O_4 magnetic particles occurs.

Adding surfactant during the preparation of the magnetic particles can allow for the control of magnetic particle growth. This is because the orientation of surfactant adsorbed on the surface of a magnetic particle can increase the retention of magnetic particles on the surface layer causing a decline in the diffusion rate and can prevent the precipitation of magnetic particles during surface deposition. The surface deposition rate slows down considerably, which can effectively control the growth of magnetic particles. Surfactant adsorption onto magnetic particles can also prevent or delay the oxidation of magnetic particles. However, excessive surfactant will result in adhesion between surfactant coatings. With too little surfactant, the coating would not be complete and the particle surface will not form a complete single-molecule adsorption layer (sometimes double-molecular adsorption layer). Therefore, a complete spherical elastic shell of surfactant will not be produced [30]. By a comparative analysis of experimental results, we chose oleic acid as a surfactant for the surface modification of nano-Fe_3O_4 particles and for 0.02 mol $FeCl_3 \cdot 6H_2O$, the optimum amount of oleic acid is 0.5 mL.

3   Conclusions

(1) For the chemical coprecipitation of nano-Fe_3O_4 magnetic particles, many factors affect the magnetic properties of the formed nano-Fe_3O_4 particles. By orthogonal design analysis and comparison of the results obtained, we found that the important factors are the Fe^{3+} to Fe^{2+} molar ratio, the reaction precursor iron salt concentration, the amount of surfactant and the amount of alkali.

(2) The optimum reaction conditions for the preparation of nano-Fe_3O_4 magnetic particles are: an Fe^{3+} to Fe^{2+} molar ratio of 1.75 using 0.02 mol $FeCl_3 \cdot 6H_2O$ dissolved in 200 mL deionized water to give a 0.1 mol/L solution and 0.5 mL surfactant with 30 mL ammonia.

(3) The other factors that have an influence are the order

of surfactant and alkali addition, aging time and stirring speed. The optimum conditions are the addition of ammonia at 60°C and heating to 80°C upon which oleic acid is added. The optimum aging time is 40–130 min and stirring speed should be close to 300 r/min.

1   Li D C. Theory and Application of Magnetic Fluid (in Chinese). Beijing: Science Press, 2003

2   Li D C, He X Z, Zhang Z L. A study of static magnetic fluid seal of large flange diameter. Magnetohydrodynamics, 2008, 44: 75–82

3   Ni X Y, Yao L F, Shen J, et al. Preparation of Nano-materials (in Chinese). Beijing: Chemical Industry Press, 2007

4   Hong R Y, Pan T T, Han Y P, et al. Magnetic field synthesis of Fe_3O_4 nanoparticles used as a precursor of ferrofluids. J Magn Magn Mater, 2007, 310: 37–47

5   Chan H T, Do Y Y, Huang P L, et al. Preparation and properties of bio-compatible magnetic Fe_3O_4 nanoparticles. J Magn Magn Mater, 2006, 304: e415–e417

6   Gaidescu R, Condurache D, Ivanoiu M. Ferrofluid with modified stabilisant. J Magn Magn Mater, 1999, 202: 197–200

7   Ren J, Shen J, Lu S C. Granule Dispersion Science and Technology (in Chinese). Beijing: Chemical Industry Press, 2005

8   Zhang Q Y, Zhang H P, Xie G, et al. Effect of surface treatment of magnetic particles on the preparation of magnetic polymer microspheres by miniemulsion polymerization. J Magn Magn Mater, 2007, 311: 140–144

9   Zheng J G, Chen Q S. Fe_3O_4 magnetic nanoparticles synthesis and characterization (in Chinese). Magn Mate Dev, 2008, 39: 36–39

10   Theophilos S I, Stylianos N. Efficiency of a solid polymer fuel cell operating on ethanol. J Power Sources, 2000, 91: 150–156

11   Du X Y, Chen Y Z, Ma Y X, et al. Alcohol-water Fe_3O_4 nanoparticles prepared by process optimization (in Chinese). Appl Chem Industry, 2008, 37: 1449–1452

12   Zhang L Y, Zhang Y F. Fabrication and magnetic properties of Fe_3O_4 nanowire arrays in different diameters. J Magn Magn Mater, 2009, 321: L15–L20

13   Fan S H, Guo X C, Liu Y J, et al. Fe_3O_4 nanocrystals simple regulation of synthesis, characterization and magnetic properties (in Chinese). Chin J Inorgan Chem, 2009, 25: 330–333

14   Wang X M, Zhang C N, Gu H C. Fe_3O_4 magnetic fluid preparation and magnetic properties (in Chinese). New Chem Mater, 2009, 37: 66–68

15   Vargas J M, Lima J E, Socolovsky L M, et al. Annealing effects on 5 nm iron oxide nanoparticles. J Nanosci Nanotechnol, 2007, 7: 3313–3317

16   Liu Y, Jiang W, Wang Y, et al. Synthesis of Fe_3O_4/CNTs magnetic nanocomposites at the liquid–liquid interface using oleate as surfactant and reactant. J Magn Magn Mater, 2009, 321: 408–412

17   Tartaj P, Morales M P, Verdaguer S V, et al. The preparation of magnetic nanoparticles for applications in biomedicine. J Phys D: Appl Phys, 2003, 36: R182–R197

18   He Y B, Qiu Z M, Qiu J M. Preparation of nano-Fe_3O_4 magnetic fluid and its properties (in Chinese). Chin J Process Engineer, 2006, 12: 263–267

19   Ganguly R, Sen S, Puri I K. Heat transfer augmentation using a magnetic fluid under the influence of a line dipole. J Magn Magn Mater, 2004, 271: 63–73

20   Roosen A, Hausner H. Techniques for agglomeration control during wet-chemical powder synthesis. Adv Ceram Mater, 1988, 3: 131–137

21   Chen T R, Sun J. Fe_3O_4 magnetic nanoparticles prepared by copre-

cipitation studies (in Chinese). Appl Chem Industry, 2009, 38: 226−232

22　Gao Q, Chen F H, Zhang J L, et al. The study of novel Fe$_3$O$_4$@γ−Fe$_2$O$_3$ core/shell nanomaterials with improved properties. J Magn Magn Mater, 2009, 321: 1052−1057

23　Chen S F, Wang Z L, Yu X P. Nano-Fe$_3$O$_4$ magnetic fluid test preparation and applied research (in Chinese). Ordnance Mater Sci Engineer, 2008, 31: 13−16

24　Zhang J S. Ultrafine Fe$_3$O$_4$ magnetic fluid preparation, characterization and stability mechanism (in Chinese). Doctoral Disseration. Jinan: Shandong University, 2003

25　Wang W M, Sun C Y. Nano-particles of rare earth magnetism on preparation (in Chinese). Chin J Rare Metals, 2007, 31: 27−31

26　Lou M Y, Wang D P, Huang W C, et al. Synthesis of nano-particle

Fe$_3$O$_4$ magnetic dispersion system in the process (in Chinese). J Build Mater, 2005, 8: 169−173

27　Kahani S A, Jafari M. A new method for preparation of magnetite from iron oxyhydroxide or iron oxide and ferrous salt in aqueous solution. J Magn Magn Mater, 2009, 321: 1951−1954

28　Hong R Y, Li J H, Li H Z, et al. Synthesis of Fe$_3$O$_4$ nanoparticles without inert gas protection used as precursors of magnetic fluids. J Magn Magn Mater, 2008, 320: 1605−1614

29　Rodrigo F C M, Cecile G, Pierre L, et al. Electro-precipitation of Fe$_3$O$_4$ nanoparticles in ethanol. J Magn Magn Mater, 2008, 320: 2311−2315

30　Zhang H P, Zhang Q Y, Zhang B L, et al. Preparation of magnetic composite microspheres by surfactant free controlled radical polymerization: Preparation and characteristics. J Magn Magn Mater, 2009, 321: 3921−3925